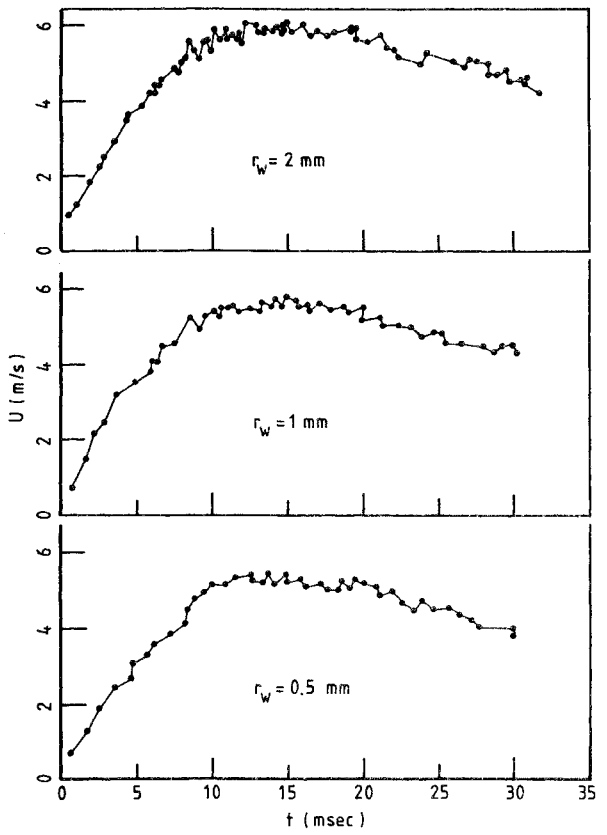

Fig. 5 Fluid velocity traces near wall boundary at $z = 153.4$ mm for short initial chamber and $P_i = 6.2$ bars.

boundary-layer thickness was found to be less than 1 mm, which corresponds to about 1% of the tube diameter. The numerical calculations of Schmitt et al.[3] predict similar boundary-layer thickness. The turbulence levels are slightly lower than those observed in the core region.

Conclusions

The main findings of this investigation are as follows:

1) The flow at any given time in the cycle is nearly one-dimensional apart from thin regions near the wall boundaries. Velocity fluctuations reach a maximum peak-to-peak value of around 6% in the core region.

2) In all cases the boundary-layer thickness is less than 1 mm, which corresponds to about 1% of the bore. The velocity fluctuations in the boundary layer are generally lower than those in the core region.

3) The velocity increases linearly with axial location from zero at the breech to that of the projectile at the base.

4) The bulk fluid velocity scales with that of the projectile, independently of initial chamber length and pressure.

Acknowledgments

The authors are pleased to acknowledge financial support provided by the U.S. Army under contract DAJA 45-84-C-0032. Useful discussions with Dr. C. Zoltani are gratefully acknowledged.

References

[1]Krier, H. and Adams, M.J., "An Introduction to Gun Interior Ballistics and a Simplified Ballistic Code," *Progress in Astronautics and Aeronautics: Interior Ballistics of Guns*, Vol. 66, edited by H. Krier and M. Summerfield, AIAA, New York, 1979, p. 1.

[2]Giovanetti, A.J. and Rife, J.M., "Internal Ballistics Model for a Liquid Monopropellant Gun," *Journal of Ballistics*, Vol. 6, No. 1, 1982, p. 1348.

[3]Schmitt, J.A., Banks, N.E., Zoltani, C.K., and Mann, T.L., "Two-Phase Viscous Flow Modeling of Interior Ballistics, Algorithm and Numerical Predictions for an Idealized Lagrange Gun," presented at the ASME Winter Annual Meeting, Washington, DC, Nov. 1981.

[4]Bicen, A.F., Kliafas, Y., and Whitelaw, J.H., "Velocity Characteristics of the Wakes of In-Cylinder Projectiles," AIAA Paper 85-1676, 1985.

Transonic Potential Flow in Hyperbolic Nozzles

Minwoo Park* and D. A. Caughey†
Cornell University, Ithaca, New York

Introduction

THE classical problem of transonic flow through a hyperbolic nozzle (see, e.g., Ref. 1) with or without a shock wave, has been revisited by applying recently developed numerical methods. Both planar and axisymmetrical cases have been considered. The full potential equation is solved in conservation form using the finite volume method of Jameson and Caughey.[2] To treat the mixed nature of the equation, either a first- or a second-order numerical viscosity in the direction of the flow is added explicitly in conservation form. A multigrid, alternating direction implicit (ADI) method[3] is used to solve the difference equations and the results are compared with analytical and numerical results of earlier researchers.

Analysis

Finite Volume Formulation

The law of conservation of mass for the isentropic flow through a nozzle can be expressed as

$$(\rho\Phi_x)_x + (\rho\Phi_y)_y = 0 \tag{1}$$

where Φ is the velocity potential and x,y Cartesian coordinates with x the axis of symmetry. Here ρ is defined as

$$\rho = \tilde{\rho} \quad \text{for planar flow}$$

$$\rho = \tilde{\rho} y \quad \text{for axisymmetric flow} \tag{2}$$

where $\tilde{\rho}$ is the fluid density which can be related to the magnitude of the velocity by the isentropic relation.

Equation (1) is transformed to a new (boundary-conforming) coordinate system (X, Y) by following the usual procedure.[2] The resulting equation can be written in terms of the contravariant velocity components (U, V) as

$$(\rho h U)_X + (\rho h V)_Y = 0 \tag{3}$$

where h is the determinant to the Jacobian matrix of the transformation.

A finite difference approximation is constructed by representing the Cartesian coordinates and the solution within each mesh cell using a bilinear mapping. Flux

Received May 9, 1985; revision received Aug. 29, 1985.

*Graduate Research Assistant, Sibley School of Mechanical and Aerospace Engineering. Student Member AIAA.

†Professor, Sibley School of Mechanical and Aerospace Engineering. Associate Fellow AIAA.

balances in the computational domain are formulated by first evaluating the flow quantities at the center of each mesh cell and then averaging these values to calculate the fluxes across the faces of auxiliary cells located midway between the grid lines. With introduction of the averaging and differencing operators μ and δ, the resulting finite difference approximation to Eq. (3) can be written as

$$\mu_Y \delta_X (\rho h U) + \mu_X \delta_Y (\rho h V) = 0 \tag{4}$$

The scheme is stabilized in supersonic regions by the addition of numerical viscosity terms that introduce an upwind bias into the difference equations. Following Caughey and Jameson,[4] this can be done in a manner that reduces the accuracy of the scheme to first order or maintains second-order accuracy everywhere except near the shock waves.

Modification of Flux Balance Equation on the Axis

For axisymmetric flow, Eq. (1) can be written as

$$(\rho\Phi_x)_x + (\rho\Phi_y)_y + \rho\Phi_y/y = 0 \tag{5}$$

Near the axis, the velocity component Φ_y goes to zero and the last term in Eq. (5) becomes indeterminate. The radial flux component at the surface of a cylindrical mesh cell around the axis having radius R can be expanded in a Taylor series as

$$\rho\Phi_y = (\rho\Phi_y)_0 + R(\rho\Phi_y)_y + \ldots \tag{6}$$

Since $(\rho\Phi_y)_0 = 0$, Eq. (5) becomes

$$(\rho\Phi_x)_x + 2(\rho\Phi_y)_y = 0 \tag{7}$$

which is valid on the axis. The finite volume equation for the corresponding flux balance on the axis can be written as

$$\mu_Y \delta_X (\rho h U) + 2\mu_X \delta_Y (\rho h V) = 0 \tag{8}$$

Grid Generation and Boundary Conditions

For the hyperbolic nozzle geometry considered here, a simple conformal mapping enables us to define a boundary-conforming coordinate system. If we let $z = x + iy$ and $\zeta = \xi + i\eta$ represent the coordinate systems in the physical and computational planes respectively, then the transformation can be written as

$$z = A\sinh(B\zeta) \tag{9}$$

where the real numbers A and B determine the nozzle shape. The grid in the physical plane is obtained by transforming a uniform mesh from the computational domain.

The use of a boundary-conforming grid greatly simplifies treatment of the boundary conditions. On the wall and centerline, no-flux boundary conditions are enforced. For example, if $j = KY$ represents the nozzle wall, the finite volume expression for the boundary condition there can be implemented by defining

$$(\rho h V)_{i,KY+\frac{1}{2}} = -(\rho h V)_{i,KY-\frac{1}{2}} \tag{10}$$

Similar expressions hold for the centerline.

When both end boundaries of the computational domain are subsonic, the value of the potential itself can be specified. Thus, if $i = 1$, and MX represents these boundaries,

$$\Phi_{1,j} = 0, \qquad \Phi_{MX,j} = \Phi_{\text{limit}} \tag{11}$$

When the flow at the downstream boundary is supersonic, the potential values at the boundary must be determined as part of the solution. But, since even at supersonic points the present scheme is implicit in the streamwise direction, downstream data are required. This is provided by extrapolating the velocity potential along each computational line. Numerical experiments have shown a cubic extrapolation scheme to result in the best convergence.

Iterative Solution

The resulting difference equations are solved using the multigrid ADI method developed by Jameson.[3] The solution procedure requires inversion of a pentadiagonal matrix along each line, in each coordinate direction, for each sweep. The multigrid algorithm was employed to accelerate convergence. A von Neumann stability analysis of the ADI scheme has been performed. Numerical evaluation of the amplification factor has shown regions of instability for selected low-wave-number disturbances when the flow is locally supersonic and inclined at intermediate angles (larger than 7, but less than 45 deg) to the grid line. In practice, this instability can be avoided by using a carefully generated grid that conforms

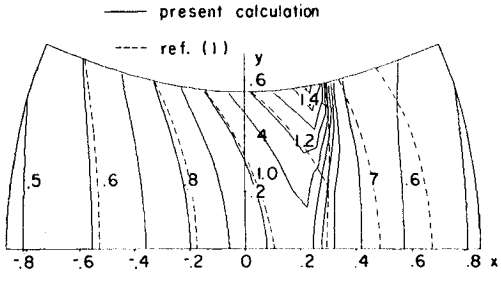

Fig. 1 Mach number contours for transonic flow in planar nozzle.

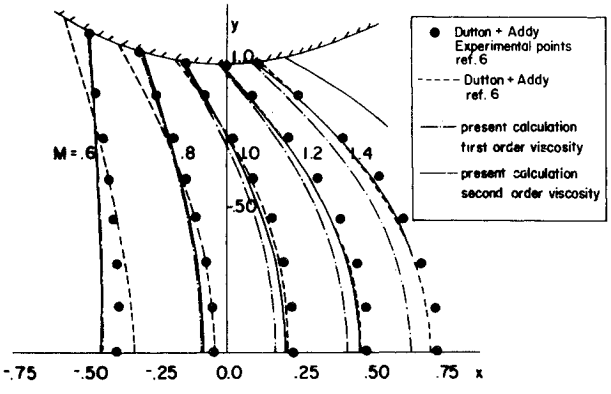

Fig. 2 Mach number contours for transonic flow in axisymmetric nozzle.

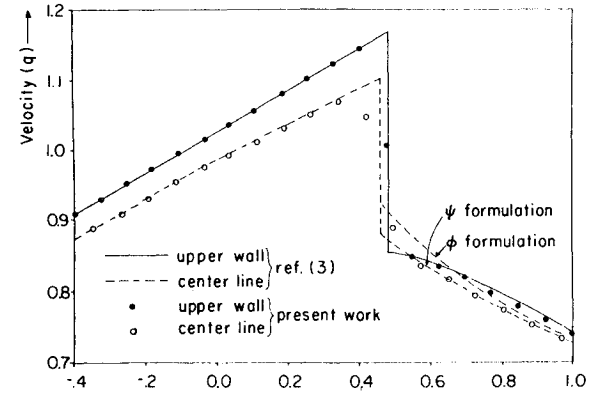

Fig. 3 Wall and centerline velocity distributions for axisymmetric nozzle flow with shock wave.

relatively well with the final shape of the streamlines. Details of the stability analysis and other aspects of the numerical scheme can be found in Ref. 5.

Results

For the present calculations, grids having 32×8 mesh cells were used. The convergence rates for both planar and axisymmetric cases were 0.92-0.95 per work unit, where one work unit corresponds to the computational time required for a single ADI sweep on the finest grid. The global features of the solution typically have converged within approximately 30 work units; such a computation requires 4.5 s of CPU time on the IBM 370/168 computer.

Results for the transonic flow through a planar nozzle are presented in Fig. 1. For this case, the nozzle throat radius is 1.82 and the boundary conditions are such that a shock wave spans the entire nozzle. Mach number contours for this case are plotted and are compared with those of Emmons[1] for the same case. Emmons used a primitive form of relaxation method that is essentially equivalent to the present method for subsonic flows. However, Emmons used a trial-and-error method for fitting the shock instead of capturing it. He also included the effects of the entropy jump and the vorticity field generated by the shock, which is the primary difference from the present method. To compare the two results, the shock position at the wall is matched by adjusting the potential value on the downstream boundary in the present calculation. There is some discrepancy between the two solutions downstream of the shock, which almost certainly can be attributed to the effect of the entropy jump included in Emmons' calculation.

In Fig. 2, results for the fully expanded flow through an axisymmetric nozzle are compared with those of Dutton and Addy.[6] They solved for a circular arc nozzle geometry with unit radius of curvature, and both the experimental and computed results are presented. Since Dutton and Addy used a perturbation method of third order, their results are independent of the precise wall shape near the throat. To minimize the effects of the geometric differences, a short domain was chosen for the present calculation; the termination of the contours for the present calculation near the downstream boundary reflects the location of the boundary of the computational domain. The basic features of the flow are essentially the same for both methods, with particularly good agreement in the throat region. As might be expected, better agreement is obtained throughout the supersonic region when using the second-order accurate form of the viscosity.

Finally, a comparison between the present work and an analytical solution for a flow containing a shock is presented. Lin and Shen[7] have obtained analytical solutions for two-dimensional and axisymmetric transonic flows in slender hyperbolic nozzles including shock waves. Their matched asymptotic analysis was carried out using expansions for both the velocity potential and stream function formulations of the equations of motion. Because the expansions used in these calculations were necessarily truncated, the results from the two formulations are slightly different. In Fig. 3, the velocity distributions along the wall and the axis of symmetry are shown for the case of a radius of curvature at the throat equal to 10. It is interesting to note that the present results match more closely with the analytical solutions for the stream function formulation than for the velocity potential formulation. This may be explained by the fact that the stream function formulation keeps the mass flow exactly constant, as does the present formulation. The shock shapes for both formulations are in good agreement with the results of the present calculations.

Conclusion

Transonic flows in hyperbolic nozzles have been calculated using a finite volume, transonic potential method. A multigrid ADI method was used to solve the resulting difference equations. The scheme converges rapidly, and results are in good agreement with those of earlier workers, including analytical results for flows containing shock waves.

Acknowledgment

This work was supported in part by the NASA Lewis Research Center under Grant NAG 3-19.

References

[1]Emmons, H. W., "The Theoretical Flow of a Frictionless, Adiabatic, Perfect Gas inside a Two-Dimensional Hyperbolic Nozzle," NACA TN 1003, 1946.

[2]Jameson, A. and Caughey, D. A., "A Finite-Volume Method for Transonic Potential Flow Calculations," *Proceedings of the AIAA 3rd Computational Fluid Dynamics Conference*, Albuquerque, NM, AIAA, New York, 1977, pp. 33-54.

[3]Jameson, A., "Acceleration of Transonic Potential Flow Calculations on Arbitrary Meshes by the Multiple Grid Method," *Proceedings of AIAA 4th Computational Fluid Dynamics Conference*, Williamsburg, VA, AIAA, New York, 1979, pp. 122-146.

[4]Caughey, D. A. and Jameson, A., "Basic Advances in the Finite-Volume Method for Transonic Potential Flow Calculations," *Numerical and Physical Aspects of Aerodynamic Flows*, edited by T. Cebeci, Springer-Verlag, New York, 1981.

[5]Park, M., "Numerical Computation of Steady Transonic Flow through Hyperbolic Nozzles," M.S. Thesis, Cornell University, Ithaca, NY, 1983.

[6]Dutton, J. C. and Addy, A. L., "Transonic Flow in the Throat Region of Axisymmetric Nozzles," *AIAA Journal*, Vol. 19, June 1981, pp. 801-804.

[7]Lin, C. Q. and Shen, S. F., "Analysis of Transonic Flow with Shocks in Slender Hyperbolic Nozzles," AIAA Paper 82-0160, 1982.

Vorticity with Variable Viscosity

Gustave J. Hokenson*
The Hokenson Company, Los Angeles, California

THE formulations developed in Ref. 1 are eminently useful in the analysis of vorticity mechanics in complex flows. As noted therein, the focus of the study was not viscous compressible flow. However, some of the equations retain the viscosity inside various derivatives, implying that all the variable viscosity effects are accounted for, at least formally. The purpose of this Note is to document some effects of the additional terms required to complete the formulation when variable viscosity flow is the subject of interest.

Following the notation in Ref. 2, the equations of motion may be written in the following form:

$$\rho \mathrm{D}u_i/\mathrm{D}t = \rho F_i - \frac{\partial p}{\partial x_i} + \frac{\partial}{\partial x_j}\left\{2\mu\left(e_{ij} - \frac{1}{3}\Delta\delta_{ij}\right)\right\} \tag{1}$$

where e_{ij} is the symmetric part of the deformation

$$e_{ij} \equiv \frac{(\partial u_i/\partial x_j + \partial u_j/\partial x_i)}{2} \tag{2}$$

$\Delta \equiv e_{ij}$ and δ_{ij} is the Kronecker delta. Density, vorticity, velocity, normal stress, body force, and the coefficient of viscosity are assigned their traditional nomenclature.

Submitted June 7, 1985; revision received Sept. 21, 1985.

*Chief Scientist. Member AIAA.